

**Research Article**

Vibration reduction on a cantilever Timoshenko beam control subjected to combined effects of wind and earthquake loads using damped outriggers

Jules Metsebo ^{a*} , Buris Peggy Ndemanou ^b , Andre Cheage Chamgoue ^c  and
Guy Richard Kol ^{b,c} 

^aDepartment of Hydraulics and water Management, National Advanced School of Engineering, University of Maroua, P.O Box 46 Maroua, Cameroon

^bDepartment of Mechanical Petroleum and Gas Engineering, Faculty of Mines and Petroleum Industries, University of Maroua; P.O Box 08 Kaélé, Cameroon

^cSchool of Geology and Mining Engineering, University of Ngaoundere, P.O. Box 115, Meiganga, Cameroon

ARTICLE INFO**Article history:**

Received 05 February 2021

Revised 01 April 2021

Accepted 20 April 2021

Keywords:

Fuzzy Logic

Method of lines

MR dampers

Outriggers

RMS

Timoshenko beam

ABSTRACT

This paper deals with the combined effects of wind and earthquake on the dynamic response of a cantilever structure. It is mainly composed of the core-structure, multi-outriggers with magnetorheological (MR) dampers localized at different levels along of the structure and perimeter columns. These control devices are semi-active in nature and exhibit a nonlinear behavior. One of their interesting characteristics is their ability to add supplementary energy dissipation to the structural system. Exposed to combined wind and earthquake loads, the core-structure is modelled using a Timoshenko cantilever beam. The stochastic approach based on the statistic properties is employed to estimate the degree excitations of the two natural hazards. The peak Root-Mean-Square (RMS) are evaluated to quantify the optimal location of damped outriggers. Defined as the control algorithm based on human reasoning, the Fuzzy logic is used to select the appropriate current that feeds the control devices. The obtained results indicate that the application of the fuzzy logic further minimizes the effects of bending-moment and shear force. All of these enhance the performance of the whole structural response and lead to a significantly reduction of excessive vibration to an acceptable level.

© 2021, Advanced Researches and Engineering Journal (IAREJ) and the Author(s).

1. Introduction

Many structural engineering structures, such as bridges, tall-buildings [1,2,40], railways [3] and nuclear power plants [4] around the world, still suffer from the vibrations induced by winds or earthquakes during their lifetime. In recent decades, these mentioned natural disturbances are considered as the most destructive. They are able to alter the physical property of the majority of infrastructures by causing the severe structural damage and human life losses. Generally, the dynamic loads of these natural phenomenon are applied in two directions (horizontal and vertical motions) along the engineering structures. Due to its effect on the performance of the structural system, the horizontal

movement has proven to be of a great importance for the design of the structural engineering [5].

To further increase the ability and resiliency of tall buildings to withstand against the external perturbations, the outrigger systems were developed in the tall buildings as an alternative solution [6]. Some cases of application of these structures already exist in Shanghai with a height of 632 meter [7] and The Burj Khalifa in Dubai with the height of 828 meters [8]. In a traditional design, this system is constituted of the core-structure characterizing the tall building behaviour, the outriggers associated with control devices and the perimeter columns. Hence, the understanding of this design has considerably increased the

* Corresponding author. Tel.: +237-699-484-135.

E-mail addresses: jmetsebo@gmail.com (J. Metsebo), ndemanoupeggy@gmail.com (B. P. Ndemanou), cham6ko@yahoo.fr (A. C. Chamgoue), kolguy_r@yahoo.fr (G. R. Kol)

ORCID: 0000-0002-4312-6856 (J. Metsebo), 0000-0003-2254-9830 (B. P. Ndemanou), 0000-0002-7422-8839 (A. C. Chamgoue),

0000-0002-9959-2709 (G. R. Kol)

DOI: 10.35860/iarej.875161

This article is licensed under the CC BY-NC 4.0 International License (<https://creativecommons.org/licenses/by-nc/4.0/>).

motivation of many researchers [9–11]. Huang et al. [12] proposed an analytical method to evaluate the dynamic response of a single damped outrigger system. Based on this approach, they obtained the optimal locations of outrigger to further reduce response. Yang et al. [13] used the finite element methods to assess the seismic performance. They indicated that the equivalent energy design procedure is an efficient method to design the outrigger system and helps to avoid the collapse at different levels of the earthquake. Zhou et al. [14] studied the analytical methods to investigate the earthquake response of an outrigger system. The authors applied this approach to determine the optimal location of the outrigger.

In view of further reinforcing the performance of the damped outriggers, the control devices are installed between the core-structure and perimeter columns. These control devices are either passive, active, semi-active nature. They can adjust the magnitude of the control force. A large number of theoretical and experimental studies have been done [15–19]. The results reveal that among the different types of control devices, MR dampers are a promising type. Because they include the active and passive properties and also require a low power to change the system's physical characteristic [20]. Despite all these encouraging results, they are however, characterized by an intrinsically non-linear behaviour, which can sometimes be a major disadvantage. To avoid any inconvenience, some suitable control algorithms were developed. They remedy to this situation by optimising the dynamics response of the MR dampers. In this context, one can note the algorithms such as Clipped optimal control [21,22], Bang-bang control [23,24], Lyapunov stability [25], genetic algorithm [26–28], sliding mode [29] and fuzzy logic [31–37]. In the present work, the fuzzy logic is directly applied to select the appropriate input current of the MR dampers. of the shear in investigating transverse vibrations [38]. It is defined as an extension of the Euler-Bernoulli theory [39]. It is in this way that, Ndemanou et al. examined the performance of magneto-rheological damper on the outrigger system. Their results indicated that at the position near the top of the structural system, the damper outrigger further improves the dynamic response of the structure. The drawback of aforementioned studies is the fact that the effects of outrigger dampers do not assessed on the bending moment and shearing force of the core-structure.

To analyse the structural response of the outrigger system, the core-structure is assumed to be elastic and homogeneous. Thus, Timoshenko cantilever beam will be used to model the core-structure. This model includes the rotatory inertia and the effect.

In this paper, the Timoshenko's beam formulation based on the partial differential equations is used to model the core-structure. The structural system will be subjected to combined wind and earthquake loads. It is assuming that the

perimeter columns are axially very stiff [15]. Therefore, the effect of its dynamic response will be assumed neglected during this investigation.

The aim of this study is to analyze how the different locations of damped outriggers significantly affect the bending moment, shear force and transversal displacement of the core-structure under the combination of two natural disturbances. Although, the mentioned above force occurs in a structure by further causing stresses. It is important to underline that the one of the most important points is to increase the beam's ability by dramatically reducing the undesirable vibrations.

2. Description of the Physical System

The structural system subjected to two natural hazards is schematically displayed in Figure 1. It is constituted of an elastic core-structure, the exterior columns and three damped outriggers localized at different positions x_1 , $x_1 + x_2$ and $x_1 + x_2 + x_3$ along the height of the structural system. The connection of all these elements is an effective means to work together and changing their dynamic response. In traditional configuration, the core-structure is a tall-building constituted of several floors. It is assumed as a uniform cantilever beam, so the ends are fixed at the bottom and free at the top. The damped outriggers denote the outriggers equipped of MR dampers and are assumed to be symmetrical in relation to the central line of the core-structure. The indicated control devices are mounted vertically between the core-structure and the perimeter column as shown in Figure 1. As can be seen, this whole structure is submitted to combined action of wind and earthquake loads. In the current state, only their component in the horizontal direction is considered. Hence, the wind flow presents an unsteady behaviour and distributed all along the height of the structure.

Unlike wind dynamics, the horizontal earthquake displacement also defined as a ground motion is rather applied to the base of the mechanical structure. It should be noted that in the present case, each of outriggers behaves as a rigid body. It is important to point up that the outriggers and the exterior columns have commonly a high stiffness.

3. Mathematical modelling

Varying with the coordinate along the beam and with time, the lateral displacement of the structure from equilibrium line is defined by the variable. In this case study, the influence of the perimeter columns on the dynamics of the core is not taken into consideration. As a result, the governing equation modelling the dynamics of the cantilever Timoshenko beam with damped outriggers submit to combined actions of vertical wind and horizontal earthquake loadings can be defined by the partial differential equation given as follows [26].

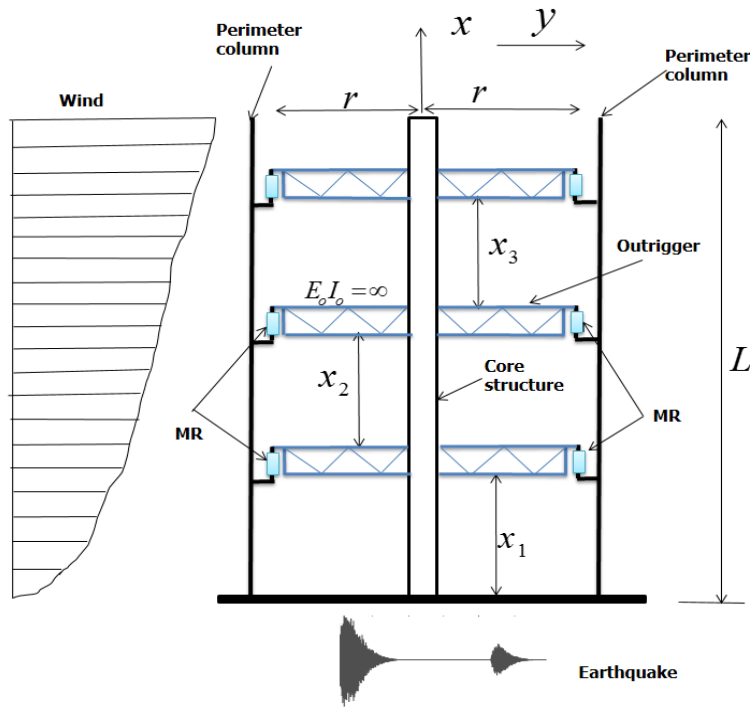


Figure 1. Schematic representation of the system under study: the simplified structure under the earthquake and wind loads

$$m \frac{\partial^2 y}{\partial t^2} + EI \frac{\partial^4 y}{\partial x^4} - mr^2 \left(1 + \frac{E}{k_s G} \right) \frac{\partial^4 y}{\partial x^2 \partial t^2} = f(x, t) - m \ddot{y}_g(t) + \frac{\partial M_a}{\partial x} \quad (1)$$

This above equation denotes transverse equation of motion. In this definition, m is the mass per unit length, ρ is the mass density of the beam, I is the moment of inertia of the cross-section area about the neutral axis, E is the elastic modulus; G is the shear modulus of elasticity. The dimensionless quantity k_s is the shear coefficient depending on the geometric of the cross-sectional area of the beam and depends on as well as of the Poisson's ratio. As indicated earlier, any information dynamics from perimeter columns linked to core-structure are not taken into account.

Note by passing that these defined geometrical characteristics are assumed constant.

Thus, within the Timoshenko theory configuration, the slope of the deflection curve ($\frac{\partial y}{\partial x}$) is the sum of the angular rotation $\psi(x, t) = \psi$ of the beam cross-section due to the bending moment. and also of the angle due to shear distortion $\gamma(x, t)$, it follows that [41].

$$\frac{\partial y}{\partial x} = \psi(x, t) + \gamma(x, t) \quad (2)$$

Consequently, the bending moment is given by Equation (3).

$$M = -EI \frac{\partial \psi(x, t)}{\partial x} \quad (3)$$

The shearing force $Q(x, t) = Q$ along the beam length by the following equation:

$$Q = k_s AG \left(\frac{\partial y}{\partial x} - \psi \right) \quad (4)$$

As stated earlier, the shearing force is a force that occurs in a structure under external loads. As a result, reducing its effects will increase the resilience of the structure.

The angular rotation mentioned in Equations (2), (3) and (4) can be obtained through the following partial equation of motion:

$$\rho I \frac{\partial^2 \psi}{\partial t^2} = E.I \frac{\partial^2 \psi}{\partial x^2} + k_s GA \left(\frac{\partial y}{\partial x} - \psi \right) \quad (5)$$

The distributed moment generated by MR dampers is [42]:

$$M_a = 2r \sum_{i=1}^3 \delta(x - x_i) f_i(t) \quad (6)$$

The symbol $\delta(x - x_i)$ denotes the Dirac Delta function and has the property given as follows

$$\delta(x - x_i) = \begin{cases} \infty & x = x_i \\ 0 & x \neq x_i \end{cases} \quad (7)$$

The subscript i indicates the different points along the core-structure. As a result, x_i in equation (7) points out the places where the damped outriggers are installed.

As mentioned earlier, the MR devices are semi-active systems and also have the capacity to add the damping to the mechanical structure. They essentially exhibit a nonlinear behavior. Thus, a great number of studies in the literature have paid attention on the understanding of different accurate mathematical models that fully describe their dynamic response [43,44]. The mathematical form proposed by Yang et al. [45] is employed in this paper. Thus, it is defined as follows:

$$f_i(t) = m_r \ddot{y}(x_i, t) + c \left(\dot{y}(x_i, t) \right) \dot{y}(x_i, t) + k_1 y(x_i, t) + \alpha_1 z_b + f_0 \quad (8)$$

z_b is an evolutionary variable given by:

$$\dot{z}_b = -\gamma_a \left| \dot{y}(x_i, t) \right| z_b |z_b|^{n_o-1} + (\delta_a - \beta_a |z_b|^{n_o}) \dot{y}(x_i, t) \tag{9}$$

Where m_r is the equivalent mass which represents the MR fluid stiction phenomenon and inertial effect; k_1 is the accumulator stiffness and MR fluid compressibility; f_0 represents the damper friction force; $c \left(\dot{y}(x_i, t) \right)$ is the postyield plastic damping coefficient, γ_a , δ_a and β_a are the shape parameters of the hysteresis loops.

The damping coefficient is considered as follows:

$$c \left(\dot{y}(x_i, t) \right) = a_b \exp \left(- \left(a_c \left| \dot{y}(x_i, t) \right| \right)^p \right) \tag{10}$$

With a_b , a_c and p are positive constants.

Note that, an overdot denotes differentiation with respect to the time variable t .

Wind is a phenomenon of great complexity due to the many flow situations resulting from the interaction of wind with structures[46]. Thus, wind-induced vibrations may cause structural damage and have devastating effects on infrastructure [47]. Thus, the mathematical model of the dynamic wind loads can be established from an aero-elastic principle. Consequently, the aero-elastic force is given by the following expression [48,49].

$$f(x, t) = \frac{1}{2} \rho_a U^2 b \left[\varepsilon_0 + \frac{\varepsilon_1}{U} \left(\frac{\partial y}{\partial t} \right) + \frac{\varepsilon_2}{U^2} \left(\frac{\partial y}{\partial t} \right)^2 + \frac{\varepsilon_3}{U^3} \left(\frac{\partial y}{\partial t} \right)^3 \right] \tag{11}$$

Where ε_j ($j = 1,2,3$) are the aerodynamic coefficients relevant to square section, ρ_a is the air mass density. U is the wind velocity which can be considered as having two components

$$U = u_1 + u_2(t) \tag{12}$$

In which u_1 denotes the mean wind velocity, representing the steady component. The velocity fluctuation component $u_2(t)$ is a time varying part representing the turbulence that defined any movement of air at speeds very great, causing particles of air to move randomly in all directions.

By inserting (11) into (12) by applying the Taylor expansion, the Equation (11) can be rewritten as follows:

$$f(x, t) = f_{w1}(x, t) + f_{w2}(x, t)u_2(t) \tag{13}$$

Where:

$$f_{w1}(x, t) = \frac{1}{2} \rho_a b \left[\varepsilon_0 u_1^2 + \varepsilon_1 u_1 \left(\frac{\partial y}{\partial t} \right) + \varepsilon_2 \left(\frac{\partial y}{\partial t} \right)^2 + \frac{\varepsilon_3}{u_1} \left(\frac{\partial y}{\partial t} \right)^3 \right]$$

and

$$f_{w2}(x, t) = \frac{1}{2} \rho_a b \left[2\varepsilon_0 u_1 + \varepsilon_1 \left(\frac{\partial y}{\partial t} \right) - \frac{\varepsilon_3}{u_1^2} \left(\frac{\partial y}{\partial t} \right)^3 \right]$$

From Equation 12, it is clearly observed that the wind-induced vibrations on the whole structure mainly present a dissipative nonlinear. Moreover, its effects depend on the temporal and spatial fluctuations along the height of the structures.

Note by passing that the effects of turbulence on structural motion stability have become an important area in wind engineering [50].

The turbulent component of the wind flow used here, is assumed by the random processes of bounded variation with multiple spectrum peaks [51]. Consequently, the corresponding form is given by the following expression:

$$u_2(t) = \sum_{j=1}^{N_1} A_j \cos[\omega_j t + \sigma_j B_j(t) + \theta_j] \tag{14}$$

Where:

A_j are positive constants representing the amplitude of bounded noise, $B_j(t)$ are mutually independent unit Wiener processes, ω_j are representing center and σ_j are mutually independent random variables uniformly distributed in range $[0, 2\pi]$.

The spectral density of u_2 defined analytically can be found as:

$$S_w(\omega) = \sum_{j=1}^{n_1} \left(\frac{A_j^2 \sigma_j^2 \left(\omega^2 + \omega_j^2 + \frac{\sigma_j^4}{4} \right)}{4\pi \left[\left(\omega^2 - \omega_j^2 - \frac{\sigma_j^4}{4} \right)^2 + \sigma_j^4 \omega^2 \right]} \right) \tag{15}$$

It should be noted that the magnitude of the spectral density can be adjusted to approximate the well-known Dryden and Von Karman spectral of wind turbulence. By modifying the values of mentioned parameters as pointed up in the reference [52].

Figure 2 displays the two-side spectral density. The mathematical expression is developed in Equation (15). This gives a view on the repartition of the energy of the bounded noise.

As mentioned earlier, the same structure is also under earthquake loads. In this configuration, the mentioned variable $\ddot{y}_g(t)$ in Equation (1) defines the seismic events characterized by the ground acceleration.

It is worth pointing out that dot denotes derivative with respect to t . Thus, the governed equations are described as follows

$$\ddot{y}_g(t) = \left(2\xi_g \omega_g \dot{x}_g(t) + \omega_g^2 x_g(t) \right) e(t) \tag{16}$$

$$\ddot{x}_g(t) + 2\xi_g \omega_g \dot{x}_g(t) + \omega_g^2 x_g(t) = w(t) \tag{17}$$

Where $x_g(t)$ is the filter response, and $w(t)$ is the stationary Gaussian white noise with the following statistics:

$$\begin{cases} \langle w(t) \rangle = 0 \\ \langle w(t)w(\tau) \rangle = 2\pi S_0 \delta(t - \tau) \end{cases} \tag{18}$$

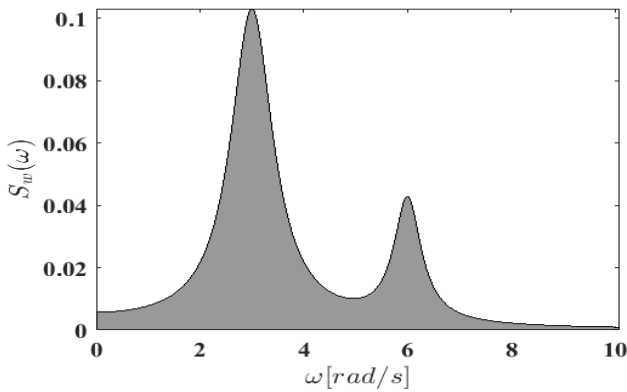


Figure 2. Spectral density of the bounded noise, with $A_1 = 0.8, A_1 = 0.4, \omega_1 = 3.0 \text{ rad/s } \omega_2 = 2\omega_1, \sigma_1 = 1.0, \sigma_2 = 0.8$

S_0 is the constant power spectral intensity of noise. $\langle \rangle$ denotes the angular brackets stand for ensemble averages [53].

The evolutionary power spectrum is given by:

$$S_g(\Omega, t) = |e(t)|^2 S_e(\Omega) \tag{19}$$

In which $e(t)$ is a deterministic envelope function of time. It is then given by the following form [54]:

$$e(t) = \begin{cases} e_{01}(t - t_1) \exp(-\lambda_1(t - t_1)) \\ 0 \\ e_{02}(t - t_2) \exp(-\lambda_2(t - t_2)) \end{cases} \tag{20}$$

Where e_{0j} and λ_j are positive constants that control intensity and non-stationary trend of the j th acceleration sequence.

The spectral density for the ground acceleration is defined as follows [55]:

$$S(\Omega) = S_0 \frac{\omega_g^4 + 4\xi_g^2 \omega_g^2 \Omega^2}{(\omega_g^2 - \Omega^2)^2 + 4\xi_g^2 \omega_g^2 \Omega^2} \tag{21}$$

Where ω_g is the dominant frequency of the soil, and ξ_g is the associated damping ratio of the soil layer.

4. Modal Equations and Numerical Results

To transform the partial form of the Equation (1) in the modal expression, let us consider the new dimensionless variables defined as follows:

$$X = \frac{x}{L}, \bar{u}_1 = \frac{u_1}{u_c}, a_1 = \frac{EI}{mL^4}, a_2 = \frac{r^2}{L^2} \left(1 + \frac{E}{k_s G} \right),$$

$$a_3 = \frac{E}{\rho L^2 \Delta X^2}, a_4 = \frac{k_s GA}{\rho I}, F(X, t) = \frac{1}{mL} f(x, t),$$

$$M^* = \frac{M_a}{mL^2}, \ddot{Y}_g = \frac{\ddot{y}_g}{L}, S_3 = \frac{\rho_a b \varepsilon_2 L b_5}{2m \times den}, S_4 = \frac{\rho_a b \varepsilon_3 L^2 b_6}{2m u_1 \times den},$$

$$S_5 = \frac{\rho_a b \varepsilon_0 u_c \bar{u}_1 b_4}{mL \times den}, S_6 = \frac{\rho_a b \varepsilon_1 b_1}{2m \times den}, S_7 = \frac{\rho_a b \varepsilon_3 L^2 b_6}{2m u_1^2 \times den},$$

$$\omega^2 = \frac{a_1 b_3}{den}, \eta_j = \frac{\phi'(X_j)}{den}, \zeta_a = \frac{2r}{L}, Z = \frac{z}{L}, \beta_L = \beta_a L^n$$

$$\gamma_L = \gamma_a L^n, den = b_1 - a_2 b_2 + \zeta_a \mu_m \sum_{j=1}^3 \phi(X_j) \phi'(X_j)$$

$$\mu_m = \frac{m_r}{mL}, f_a = \frac{1}{mL^2} f_0, \alpha_m = \frac{1}{mL} \alpha_l, K_1 = \frac{1}{mL} k_1,$$

$$C = \frac{1}{mL} c,$$

According to the relationships between the parameters, these leads to rewrite the Equation (1) of the dynamic of the structural system under the form:

$$\frac{\partial^2 Y}{\partial t^2} + a_1 \frac{\partial^4 Y}{\partial X^4} - a_2 \frac{\partial^4 Y}{\partial X^2 \partial t^2} = F(X, t) - \ddot{Y}_g(t) + \frac{\partial M^*}{\partial X} \tag{22}$$

It can be seen that the dimensionless expression only affects the spatial variable.

By considering that the transverse deflection of the beam can be written in term of product of two variables in the following form

$$Y = \phi(X)z(t) \tag{23}$$

In which, the function $\phi(X)$ is the spatial expression, $z(t)$ is the evolutionary displacement. Thus, the scheme for obtained this form has been detailed recently in reference [25]. In this paper, only the fundamental mode is considered because it contains more vibrational energy of the structural system.

By taking into account the internal damping, the mathematical manipulation of Equations (22) and (23) leads to modal equation given as:

$$\ddot{z} + \beta \dot{z} + \omega^2 z(t) = s_1 + s_2 \dot{z} + s_3 (\dot{z})^2 + s_4 (\dot{z})^3 + (s_5 + s_6 \dot{z} - s_7 (\dot{z})^3) u_2(t) - \sigma \ddot{Y}_g + \zeta_a \sum_{i=1}^3 \eta_i F_{m_i}(t) \tag{24}$$

From equation (24) it is well understood that, unlike seismic action, the effects of wind action on the structure increase the lateral deformation. Consequently, the mechanical system exhibits a nonlinear dynamic. This is due to the presence of nonlinear damping terms.

The dimensionless damping force of the control devices $F_{m_i}(t)$ can be written as follows:

$$F_{m_i}(t) = C (\dot{z} \phi(X_i)) \dot{z} \phi(X_i) + K_1 z \phi(X_i) + \alpha_m Z_{bi} + f_a$$

and

$$\dot{Z}_{bi} = -\gamma_L |\phi(x_i) \dot{z}| Z_{bi} |Z_{bi}|^{n-1} + (\delta_a - \beta_L |Z_{bi}|^n) \phi(x_i) \dot{z} \tag{25}$$

The damping coefficient can be rewritten as follows:

$$C (\dot{z} \phi(X_i)) = a_b^* \exp \left(- (a_c^* |\dot{z} \phi(X_i)|)^p \right)$$

To defined angular rotation the method of lines or semi-discretization method is applied on the Equation (5). It is a method is a procedure for obtaining the solution of the partial differential equations. This discretization approach is generally applied on the spatial variables. As a result, the Equation (5) can be expressed as:

$$\ddot{\psi}_n = a_3 (\psi_{n+1} - 2\psi_n + \psi_{n-1}) + a_4 (\phi'(x_n) z(t) - \psi_n) \tag{26}$$

The dimensionless boundary conditions can be written as follows:

$$X = 0 \rightarrow \psi_n = 0,$$

$$X = 1 \rightarrow \psi_{n+1} = \psi_{n-1}$$

This iteration method well-known in the literature is used to have the behavior of the system during the temporal evolution.

The core-structure considered in this study is assumed to have a total height $L = 300$ m. Its intrinsic properties are: Young’s modulus E of the material is 210 GPa, The shear Modulus of elasticity is $G = 81$ GPa, Poisson’s ratio ν is 0.3. The geometric properties are: mass of the core is $2 \times 10^5 \frac{kg}{m}$. The cross-section corresponds to $12 \text{ m} \times 12 \text{ m}$, thickness is 0.5 m and the shear coefficient $k_s = 0.435$. For the nonstationary ground acceleration, The intensities of the acceleration sequences at the first and second sequences $S_0 = 0.02 \text{ m}^2/\text{s}^3$ and $S_0 = 0.015 \text{ m}^2/\text{s}^3$, respectively. The parameters of the envelope functions are adopted as $e_{01} = 0.8155\lambda_1 = 0.3 \text{ s}^{-1}$ and $e_{02} = 0.9514$, $\lambda_2 = 0.35 \text{ s}^{-1}$ and the separating time interval between the sequences is 15 s. The interval time of the envelope function are $t_1 = 25 \text{ s}$, $t_2 = 40 \text{ s}$, $t_3 = 60 \text{ s}$.

Regarding the control devices, some of parameters are summarized in Table 1 [44]. These MR devices are able to generate the larger damping force [56]. Hence, in the present investigation, some values of parameters illustrated in Table 1 will be adjusted in order to have the appropriate values which defines a large-scale control device. From such devices are able to attenuate excessive vibrations of the structure under the optimal conditions. There are other parameters which do not depend on the input current and are therefore given by:

$$\gamma_a = 5179.04 \text{ m}^{-1}, \delta_a = 1377.9788,$$

$$\beta_a = 27.1603 \text{ m}^{-1}, p = 0.2442, k_1 = 20159.5 \text{ N/m}$$

It is interesting to indicate that the MR damper can be implemented in passive-off or passive-on mode. For each mode considered herein, the peak RMS of the shear force and bending-moment of the core-structure under combined wind and earthquake loads will be calculated to research to reasonable optimal location of the damper outriggers. Let us remind the readers that in configuration of the

outrigger system, one cannot refer our analysis to the comparison of controlled and uncontrolled cases. Because the damper outriggers are rigidly linked to core-structure and perimeter columns.

4.1 Passive-off

The passive off means the input current is zero. In other words, the MR damper is employed as a passive option. To assess the dynamic response of the structural system in this mode, the values of the control device will be selected in the first row in Table 1.

The next step is to apply the appropriate algorithm to numerically solve the Equations (24)-(26). Let us consider four positions of the damped outriggers defined as follows:

$$OL_1 = (0.4; 0.6; 0.8) ; OL_2 = (0.2; 0.7; 0.9) ; OL_3 = (0.3; 0.5; 0.9); OL_4 = (0.4; 0.7; 0.9).$$

Hence, it is worth investigate how the mentioned various positions of damper outriggers affect the shear force and bending-moment. The goal is to find the optimal position.

For this case, the length of an outriggers is $r = 4.0$.

Figure 3 and 5 clearly show the peak RMS of bending-moment and shear force at each point along of the core-structure, respectively. It appears that its different positions of damped outriggers rigidly connected to the core-structure affect significantly the moment-bending and shear force.

The results presented in Table 2 show that the bending-moment is very low at the point 0.1 of the core-structure and is high at the rest of points (0.2 up to 0.9) of the beam. It comes out that whatever the damped outriggers the value of the bending-moment is important at the point 0.3 of the mentioned structure. Looking closely at in Table 2, it is observed that the bending-moment is slightly small at location OL_4 compared to OL_1 , OL_2 and OL_3 .

The peak RMS values of the shear force in Figure 4 are shown in Table 3. The results indicate that the shear force is significantly important at the point 0.1 of the core-structure compared to the other points. The effects of the OL_4 of the damper outriggers are clearly weak on the core-structure than OL_1 , OL_2 and OL_3 .

Table 1. Damper parameter at various current levels

Current(A)	$\alpha_l(10^8 N)$	$\alpha_b(10^3 Ns/m)$	$a_b(10^3 s/m)$	$m_r(10^3 kg)$	no	$f_0(10^3 N)$
0.0237	1.3612	4,349,000	862.03	3,000	1.000	1,465.82
0.2588	2.2245	24,698,000	3,677.01	11,000	2.0679	2,708.36
0.5124	2.3270	28,500,000	3,713.88	16,000	3.5387	4,533.98
0.7625	2.1633	32,488,000	3,849.91	18,000	5.2533	4,433.08
1.0132	2.2347	24,172,000	2,327.49	19,500	5.6683	2,594.41
1.5198	2.2200	38,095,000	4,713.21	21,000	6.7673	5,804.24
2.0247	2.3002	35,030,000	4,335.08	22,000	6.7374	5,126.79

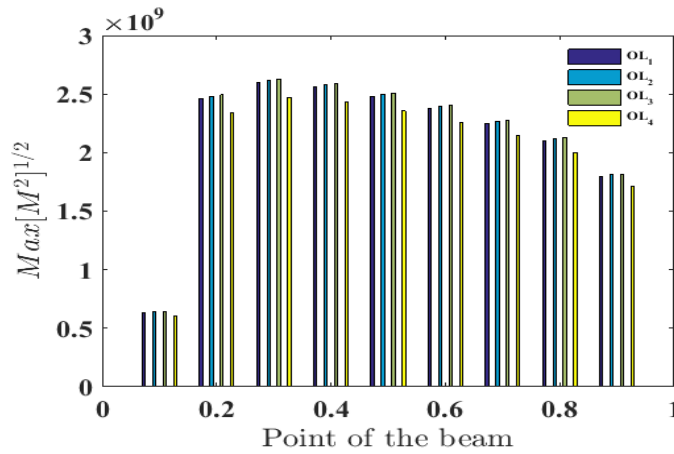


Figure 3. Peak RMS of bending moment at different points of the beam

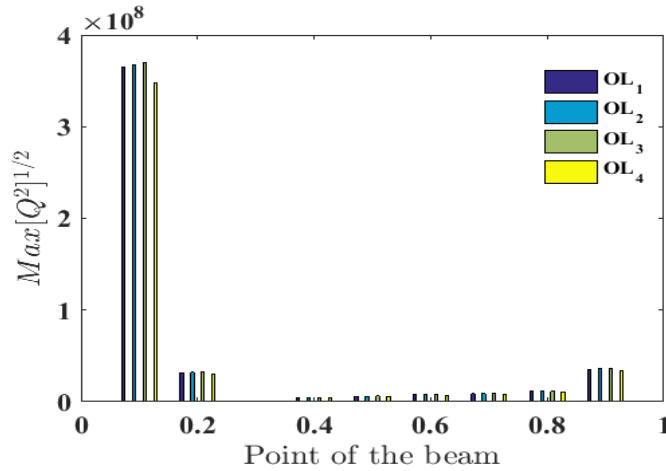


Figure 4. Peak RMS of shear force at different points of the beam

Table 2. Various peak values of RMS of the bending-Moment function of locations of damper outriggers.

$Max[M^2]^{1/2} \times 10^8$									
Outrigger location	Point of the beam								
	0.1	0.2	0.3	0.4	0.5	0.6	0.7	0.8	0.9
<i>OL₁</i>	6.34	24.64	25.98	25.58	24.78	23.74	22.51	21.02	17.96
<i>OL₂</i>	6.39	24.82	26.18	25.77	24.97	23.97	22.68	21.18	18.09
<i>OL₃</i>	6.42	24.93	26.29	25.88	25.08	24.03	22.78	21.27	18.18
<i>OL₄</i>	6.03	23.43	24.72	23.34	23.58	22.59	21.42	20.00	17.09

Table 3. Different peak values of RMS of the shear force in relation to locations of damper outriggers.

$Max[Q^2]^{1/2} \times 10^7$									
Outrigger location	Point of the beam								
	0.1	0.2	0.3	0.4	0.5	0.6	0.7	0.8	0.9
<i>OL₁</i>	36.53	3.18	0.025	0.42	0.61	0.76	0.87	1.14	3.56
<i>OL₂</i>	36.79	3.21	0.025	0.42	0.61	0.76	0.88	1.26	3.58
<i>OL₃</i>	36.96	3.22	0.025	0.42	0.62	0.77	0.89	1.16	3.60
<i>OL₄</i>	34.75	3.03	0.024	0.39	0.58	0.72	0.84	1.09	3.39

By summarizing the data in Table 1 and the results presented in Table 2, one can see that the location OL₄ of the damped outriggers is the optimal position. Because it

provides effective damping compared to other to reduce the bending-moment and shear force within the structural system.

4.2 Passive-on

One of the drawback associated with the MR damper is their nonlinear behaviour. It is due to its intrinsically characteristic that the appropriate algorithms used with MR damper are developed to suitable provide voltage or current that commands these control devices. Thus, in this present investigation, the fuzzy logic controller is employed to determine the appropriate output matched to inputs. According the principle of fuzzy logic, the different steps are: the fuzzification, the fuzzy inference associated with the control rules and defuzzification. The membership functions of the linguistic of inputs 1 (κ_1) and

2 (κ_2) are divided into six variables (i=1,2): Z*E*i (Zero), S*M*i (Small Medium), M*E*i (Medium), L*a*i (Large) , V*L*i (Very Large) and E*L*i (Extreme Large). Fuzzy variables defined as Z*E* (Zero), S*M* (Small Medium), M*E* (Medium), L*A*(Large) and V*L* (Very Large) are assigned to the output. The triangular and trapezoid membership functions used for all input and output are plotted. One can see that the two variables have different domain interval but having the same variables.

The fuzzy control rules are developed as shown in Table 4. The considered first set defines the RMS displacement and second one is the RMS velocity.

Table 4: Fuzzy control rules

		κ_1					
		Z <i>E</i> ₁	S <i>M</i> ₁	M <i>E</i> ₁	L <i>A</i> ₁	V <i>L</i> ₁	E <i>L</i> ₁
κ_2	Z <i>E</i> ₂	Z<i>E</i>	Z<i>E</i>	M<i>E</i>	S<i>M</i>	L<i>A</i>	V<i>L</i>
	S <i>M</i> ₂	Z<i>E</i>	S<i>M</i>	S<i>M</i>	M<i>E</i>	M<i>E</i>	L<i>A</i>
	M <i>E</i> ₂	M<i>E</i>	S<i>M</i>	M<i>E</i>	L<i>A</i>	L<i>A</i>	S<i>M</i>
	L <i>A</i> ₂	M<i>E</i>	M<i>E</i>	L<i>A</i>	L<i>A</i>	V<i>L</i>	L<i>A</i>
	V <i>L</i> ₂	M<i>E</i>	L<i>A</i>	L<i>A</i>	L<i>A</i>	V<i>L</i>	S<i>M</i>
E <i>L</i> ₂	L<i>A</i>	M<i>E</i>	V<i>L</i>	V<i>L</i>	L<i>A</i>	V<i>L</i>	

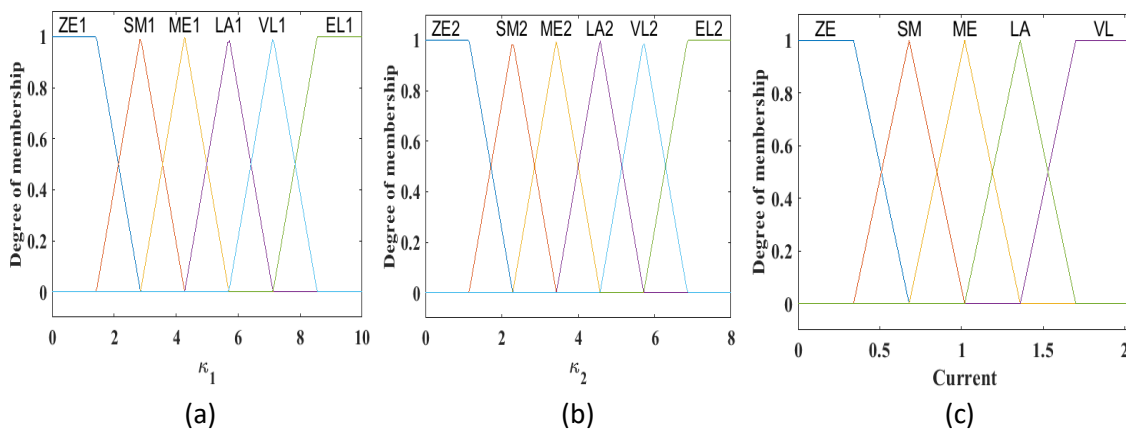


Figure 5. Membership functions for (a)-(b) inputs, (c) output

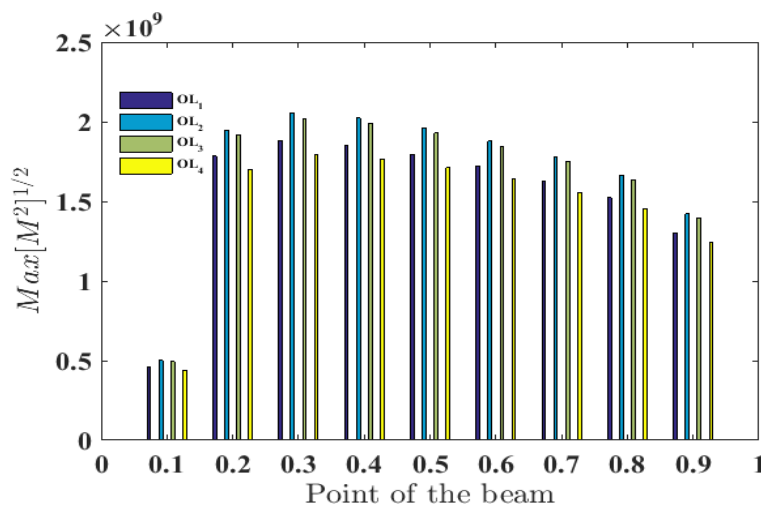


Figure 6. Peak RMS of the bending-Moment function of various points of the beam

Figure 6 shows the location effects of the damped outriggers on the bending-moment. It can be seen that the results are similar to the previous analysis. That is to say that moment is low at the point 0.1 and large at 0.3 of the core-structure.

Table 5 displays the various values of the RMS of the shear force. By focusing our attention on mentioned table, one can see that the coordinate OL₄ is still the optimal location as indicated in the previous analysis in Table 2. Because in this position the values of the bending-moment are slightly reduced than other locations. Thus, it is clearly observed that at this optimal location, the peak RMS of bending-moment is reduced up to 27% in the core-structure.

Here, the various peak RMS of the shear force in

Figure 7 are shown in Table 6. It comes out from the variation of locations of the damped outriggers affects the

shear force. Thus, the comparative data indicates that the position OL₄ of the damped outrigger further provides damping of the structural system. Therefore, it is more efficient than other position. One should be noted that the amplitude of reduction of the shear force can also reach the order of 27% in the core-structure.

To further investigate the performance of the damped outrigger on the dynamical response the whole structure. . It is important to analyze the effects of the length of the outrigger on the dynamic of the structural system.

Figure 8 and 9 present the peak RMS of the bending moment and shear force versus the various points along of the core-structure, respectively. It is observed that at the point 0.1 the bending-moment is low and large for the shear force. Although at the point 0.3 of the beam the bending-moment is rather large and very low for the shear force.

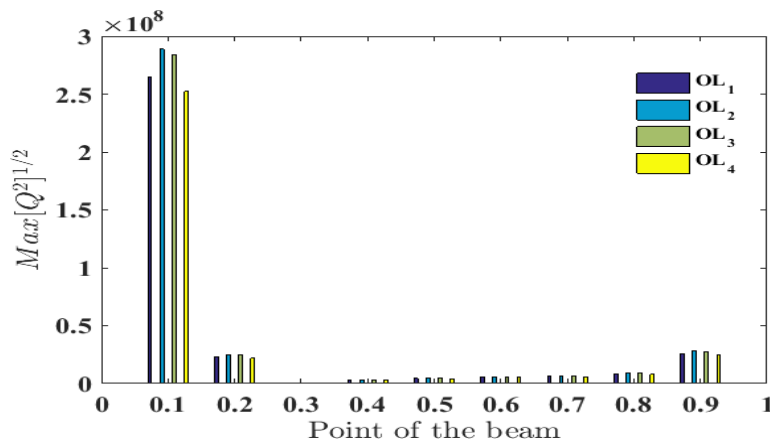


Figure 7. Peak RMS of the shear force function various points along the beam

Table 5. Peak RMS values of the bending-moment function to location of outriggers.

$Max[M^2]^{1/2} \times 10^8$									
Outrigger location	Point of the beam								
	0.1	0.2	0.3	0.4	0.5	0.6	0.7	0.8	0.9
OL ₁	4.59	17.84	18.82	18.52	17.95	17.19	16.30	15.22	13.00
OL ₂	5.01	19.48	20.55	20.23	19.60	18.78	17.80	16.63	14.21
OL ₃	4.93	19.16	20.21	19.90	19.28	18.48	17.51	16.36	13.98
OL ₄	4.38	17.01	17.95	17.67	17.12	16.40	15.55	14.52	12.41

Table 6. Peak RMS values of the shear force function to location of outriggers.

$Max[Q^2]^{1/2} \times 10^7$									
Outrigger location	Point of the beam								
	0.1	0.2	0.3	0.4	0.5	0.6	0.7	0.8	0.9
OL ₁	26.45	2.3	0.022	0.3	0.44	0.55	0.64	0.83	2.58
OL ₂	28.88	2.52	0.022	0.33	0.48	0.59	0.69	0.91	2.82
OL ₃	28.41	2.47	0.022	0.33	0.47	0.59	0.68	0.88	2.77
OL ₄	25.23	2.19	0.021	0.29	0.42	0.52	0.61	0.79	2.46

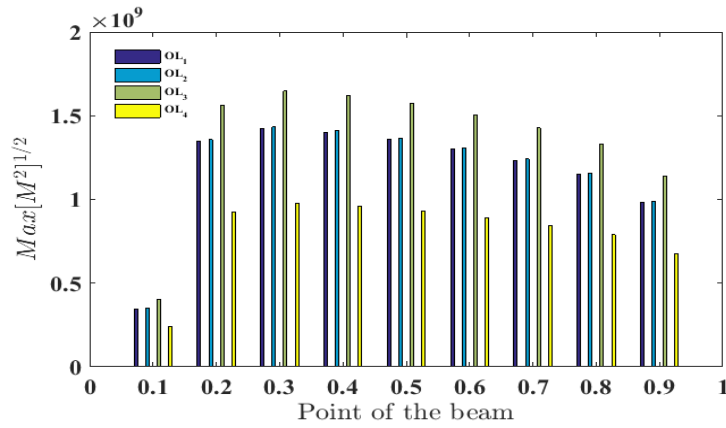


Figure 8. Peak RMS of the bending-moment function various points along the beam

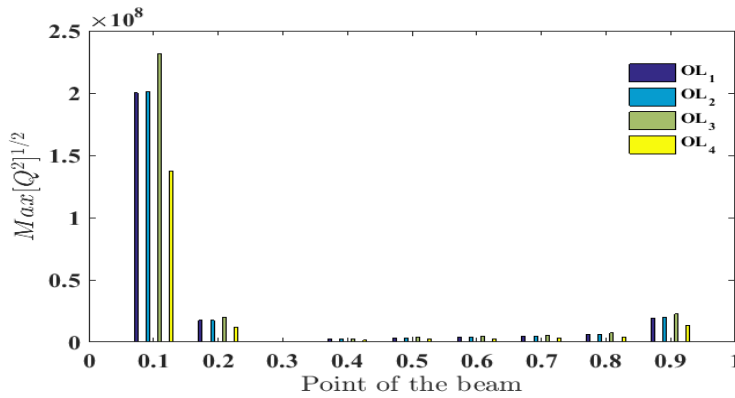


Figure 9. Peak RMS of the shear force function of various points along the beam with $r = 8.0$

Table 7 and 8 show the various peak RMS of the bending-moment and shear force in function locations of the damped outriggers, respectively. It can see that the increasing outrigger’s length can considerably reduce the bending-moment and shear force up to 45% of results from Table 5 Table 6.

Figure 10 displays outrigger’s length effects on the traversal displacement when damped outriggers are placed at the point of coordinate OL_4 . It should be noted that at this position the damped outriggers are benefits and efficient than others. It is also observed the outrigger’s length considerably affects the dynamic response of the core-structure under combined wind and earthquake loads.

Table 7: Peak RMS values of the bending-moment function to location of outriggers

$Max[M^2]^{1/2} \times 10^8$									
Outrigger location	Point of the beam								
	0.1	0.2	0.3	0.4	0.5	0.6	0.7	0.8	0.9
OL_1	3.47	13.49	14.24	14.02	13.58	13.02	12.34	11.52	9.84
OL_2	3.49	13.58	14.32	14.09	13.66	13.08	12.41	11.58	9.9
OL_3	4.02	15.61	16.72	16.22	15.71	15.06	14.27	13.33	11.39
OL_4	2.38	9.26	9.77	9.61	9.32	8.93	8.46	7.90	6.75

Table 8: Peak values RMS values of the shear force function to location of outriggers

$Max[Q^2]^{1/2} \times 10^7$									
Outrigger location	Point of the beam								
	0.1	0.2	0.3	0.4	0.5	0.6	0.7	0.8	0.9
OL_1	20.02	1.75	0.019	0.23	0.33	0.42	0.48	0.63	1.95
OL_2	20.13	1.75	0.019	0.23	0.33	0.42	0.49	0.63	1.97
OL_3	23.15	2.01	0.021	0.26	0.39	0.48	0.56	0.73	2.26
OL_4	13.73	1.19	0.017	0.16	0.23	0.29	0.33	0.43	1.34

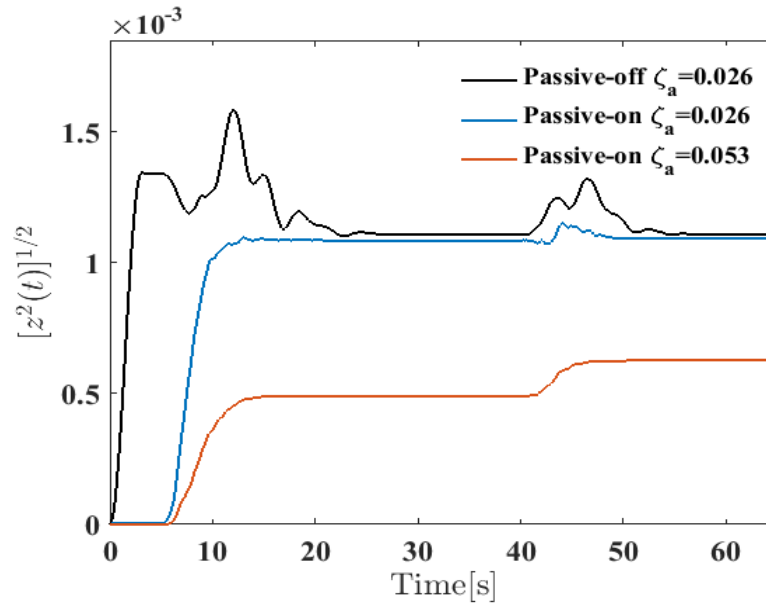


Figure 10. Variation of outrigger's length effects on RMS of displacement with the damped outriggers placed at the point OL₄

5. Discussions

The main investigation is to demonstrate how, the optimal position of damped outriggers can provide additional damping by attenuating the effects of the bending-moment and the shear force which may occur in the core-structure. Thus, to explore this phenomenon, different modes have been analysed.

In passive-off mode, the results show that the bending-moment and shear force at each point along the core-structure. It appears that this mentioned moment is significantly important at the point 0.1 and insignificant at the point 0.3 of the structure. Opposite to bending-moment, the shear force is rather insignificant at the point 0.1 and important at the point 0.3 of the core-structure. As discussed in earlier paragraph, the combined data reveal that the locations of the damped outriggers at the coordinate OL₄ further reduces the bending-moment and the shear force compared to other positions thus defined.

In passive-on mode, the Fuzzy logic algorithm used with MR damper to command the current is explored. It is observed that the application of this algorithm gradually decreases the effects of the bending-moment and shear force at any point along of the core-structure. In addition, the analysis of location effects of different damped outriggers indicates that the position OL₄ is better than OL₁, OL₂ and OL₃.

Note that the investigation of the attenuation of mentioned effects is not limited only to the two passive modes. An additional review of the length of the outrigger (geometric parameter) shows that:

- The length of the outrigger is an influencing factor, since an increasing of its value of this latter gradually decreases the effects of the moment-bending and the shear force of the core-structure;

- A significantly attenuation of the lateral deflection.

In summary, it should be noted that the passive-on mode associated with variation of the length of the outrigger compared to passive-off mode considerably reduces the moment-bending and shear force effects of the core-structure under combined wind and earthquake loads up to 60%.

6. Conclusion

This paper investigates the effects of damped outriggers placed at various locations on the bending-moment and shear force of the core structure under combined wind and earthquake loads. Timoshenko theory, based on the partial differential equation has been explored to model the core-structure. It has been observed that the wind loads have significantly introduced the nonlinear dissipative of the mechanical structure.

The effects on different locations of damped outriggers have been analysed. The numerical results have revealed that;

- In passive off mode, analysis different data of peak RMS has shown that the position OL₄ like the optimal location where the damped outriggers should be installed on the core-structure. Since in this position, the damped outriggers mitigate the induced-vibration wind and earthquake excitation better than other locations;
- In passive on mode, the dynamics of the control devices have really enhanced the response of the bending-moment and shear force in all the points of the core-structure. This is due to the application of the fuzzy logic controller

Although the two modes are explored. The influence of the length of the outriggers has also been analysed. It comes out that a slightly increasing of its length effectively

strengthens the structural composition by reducing the bending-moment and shear force effects. It can also see how this positively affects the transverse displacement of the core-structure. Additionally, this analysis of this modification shows that the optimal location of outriggers remains unchanged.

Declaration

The author(s) declared no potential conflicts of interest with respect to the research, authorship, and/or publication of this article. The author(s) also declared that this article is original, was prepared in accordance with international publication and research ethics, and ethical committee permission or any special permission is not required.

Author Contributions

J. Metsebo proposed and modeled the system. B.P. Ndemanou and A.C. Chamgoue made the numerical analysis. G.R. Kol organized and structured the manuscript.

References

- Lin YK and Yang JN, *Multimode bridge response to wind excitations*. Journal of Engineering Mechanics, 1983. **109**(2): p. 586-603.
- Gu M and Quan Y, *Across-wind loads of typical tall buildings*. Journal of Wind Engineering and Industrial Aerodynamics, 2004. **92**(13): p. 1147-1165.
- Ali AM, Alexander J and Ray T, *Frequency-independent hysteretic dampers for mitigating wind-induced vibrations of tall buildings*. Structural Control and Health Monitoring, 2019. **e2341**: p. 1-22.
- Kang X, Jiang L, Bai Y and Caprani CC, *Seismic damage evaluation of high-speed railway bridge components under different intensities of earthquake excitations*. Engineering Structures, 2017. **152**: p. 116-128.
- Kubo T, Yamamoto T, Sato K, Jimbo M, Imaoka T and Umeki Y, *A seismic design of nuclear reactor building structures applying seismic isolation system in a high seismicity region – a feasibility case study in Japan-*. Nuclear Engineering and Technologies, 2014. **46**(5): p. 581–594.
- Taranath BS, *Wind and Earthquake Resistant Buildings*, 2004, USA. CRC Press.
- Fang C, Spencer BF, Xu J, Tan P and Zhou F, *Optimization of damped outrigger systems subject to stochastic excitation*. Engineering Structures, 2019. **191**: p. 280–291.
- Zhou Y, Zhang C and Lu X, *Earthquake resilience of a 632-meter super-tall building with energy dissipation outriggers*. Proceedings of the 10th National Conference on Earthquake Engineering, Earthquake Engineering Research Institute, Anchorage, AK, 2014.
- Baker B and Pawlikowski J, *The design and construction of the World's tallest building: The Burj Khalifa, Dubai*. Structural Engineering International, 2015. **25**(4): p. 389-394.
- Lu X, Liao W, Cui Y, Jiang Q, and Zhu Y, *Development of a novel sacrificial-energy dissipation outrigger system for tall buildings*. Earthquake Engineering and Structural Dynamics, 2019. **48**: p. 1661–1677.
- Lin P and Takeuchi T, *Seismic performance of buckling-restrained brace outrigger system in various configurations*. Japan Architectural Review, 2019. **2**: p. 392–408.
- Chen Y, McFarland DM, Wang Z, Spencer BF and Bergman LA, *Analysis of tall buildings with damped outriggers*. Journal of Structural Engineering, 2010. **136**(11): p. 1435-1443.
- Huang B and Takeuchi T, *Dynamic response evaluation of damped-outrigger systems with various heights*. Earthquake Spectra, 2017. **32**(2): p. 665-685.
- Yang TY, Atkinson J, Tobber L, Tung DP and Neville B, *Seismic design of outrigger systems using equivalent energy design procedure*. The Structural Design of Tall Special Buildings, 2020. **e1743**: p. 1-15.
- Zhou Y, Xing L and Zhou G, *Spectrum Analysis-Based Model for the Optimal Outrigger Location of High-Rise Buildings*. Journal of Earthquake Engineering, 2019. p. 1-26.
- Asai T and Watanabe Y, *Outrigger tuned inertial mass electromagnetic transducers for high-rise buildings subject to long period earthquakes*. Engineering Structures, 2017. **153**: p. 404–410.
- Tan P, Fang CJ, Chang CM, Spencer BF and Zhou FL, *Dynamic characteristics of novel energy dissipation systems with damped outriggers*. Engineering Structures, 2015. **98**: p. 128-140.
- Lu Z, He X and Zhou Y, *Performance-based seismic analysis on a super high-rise building with improved viscously damped outrigger system*. Structural Control and Health Monitoring, 2018. **e2190**: p. 1-21.
- Xing L, Zhou Y and Huang W, *Seismic optimization analysis of high-rise buildings with a buckling-restrained brace outrigger system*. Engineering Structures, 2020. **220**: 110959.
- Shan J, Shi Z, Gong N and Shi W, *Performance improvement of base isolation systems by incorporating eddy current damping and magnetic spring under earthquakes*. Structural Control and Health Monitoring, 2020. **e2524**: p. 1-20.
- Ndemanou BP and Nbenjo BRN, *Fuzzy magnetorheological device vibration control of the two Timoshenko cantilever beams interconnected under earthquake excitation*. The Structural Design of Tall and Special Buildings, 2018. **e1541**: p. 1-11.
- Yoshida O and Dyke S, *Seismic control of a nonlinear benchmark building using smart dampers*. Journal of Engineering Mechanics, 2004. **130**(4): p. 386-3892.
- Zafarani MM and Halabian AM, *A new supervisory adaptive strategy for the control of hysteretic multi-story irregular buildings equipped with MR-dampers*. Engineering Structures, 2020. **217**:110786.
- Rayegani A and Nouri G, *Application of Smart Dampers for Prevention of Seismic Pounding in Isolated Structures Subjected to Near-fault Earthquakes*. Journal of Earthquake Engineering, 2020. <https://doi.org/10.1080/13632469.2020.1822230>
- Jansen L and Dyke S, *Semi-active control strategies for MR dampers: comparative study*. Journal of Engineering Mechanics, 2000. **126**(8): 795–803.
- Ndemanou BP, Fankem ER and Nana Nbenjo BR (2017) *Reduction of vibration on a cantilever Timoshenko beam subjected to repeated sequence of excitation with magnetorheological outriggers*. The Structural Design of Tall and Special Buildings, 2017. **e1393**: p. 1-10.

27. Uz ME and Hadi MNS, *Optimal design of semi active control for adjacent buildings connected by MR damper based on integrated fuzzy logic and multi-objective genetic algorithm*. Engineering Structures, 2014. **69**: p. 135-148.
28. Braz-César MT, Folhento PLP and Barros RC, *Fuzzy controller optimization using a genetic algorithm for non-collocated semi-active MR based control of a three-DOF framed structure*. 13th APCA International Conference on Control and Soft Computing, CONTROLO, 2018.
29. Bozorgvar M and Zahrai SM, *Semi-active seismic control of buildings using MR damper and adaptive neural-fuzzy intelligent controller optimized with genetic algorithm*. Journal of Vibration and Control, 2019. **25**(2): p. 1-13.
30. Moon SJ, Bergman LA and Voulgaris PG, *Sliding mode control of cable-stayed bridge subjected to seismic excitation*. Journal of Engineering Mechanics, 2003. **129**(1): p. 71-78.
31. Ghaffarzadeh H, *Semi-active structural fuzzy control with MR dampers subjected to near-fault ground motions having forward directivity and fling step*. Smart Structures and Systems, 2013. **12**(6): p. 595-617.
- 32.** Kim HS, *Seismic response reduction of a building using top-story isolation system with MR damper*. Contemporary Engineering Sciences, 2014. **7**(21): p.979-986.
33. Ok SY, Kim DS, Park KS and Koh HM, *Semi-active fuzzy control of cable-stayed bridges using magneto-rheological dampers*. Engineering Structures, 2007. **29**(5): p. 776-788.
34. Ab Talib MH and Mat Darus IZ, *Intelligent fuzzy logic with firefly algorithm and particle swarm optimization for semi-active suspension system using magneto-rheological damper*. Journal of Vibration and Control, 2016. **23**(3): p. 501-514.
35. Li Z, Yang Y, Gong X, Lin Y, and Liu G, *Fuzzy control of the semi-active suspension with MR damper based on μGA* , IEEE Vehicle Power and Propulsion Conference Harbin, China, (VPPC '08), 2008. p. 1–6.
36. Dong XM and Yu M, *Genetic algorithm based fuzzy logic control for a magneto-rheological suspension*. Journal of Vibration and Control. 2014. **20**: p. 1343–1355.
37. Paksoy M, Guclu R and Cetin S, *Semiaactive self-tuning fuzzy logic control of full vehicle model with MR damper*. Advances in Mechanical Engineering. 2014. **6**:816813.
38. Timoshenko SP, *On the correction for shear of the differential equation for transverse vibrations of prismatic bars*. The London, Edinburgh, Dublin Philosophical Magazine and Journal of Science, 1921. **41**(215): p. 744–746.
39. Hutchinson JR, *Transverse vibrations of beams, exact versus approximate solutions*. Journal of Applied Mechanics, 1981. **48**(4):923.
40. Saeid F and Bahadır Yüksel S, *Investigation of nonlinear behavior of high ductility reinforced concrete shear walls*. International Advanced Researches and Engineering Journal, 2020. **04**(02): p. 116-128.
41. Kelly SG, *Advanced vibration analysis*, USA, 2006. CRC Press.
42. Deng K, Pan P, Lam A and Xue Y, *A simplified model for analysis of high-rise buildings equipped with hysteresis damped outriggers*. The Structural Design of Tall and Special Buildings, 2013. **23**(15): p. 1158-1170.
43. Spencer BF, Dyke SJ, Sain MK and Carlson JD, *Phenomenological model for magnetorheological dampers*. Journal of Engineering Mechanics, 1997. **123**(3): p. 230-238.
44. Yang G, Spencer BF, Carlson JD and Sain MK, *Large-scale MR fluid dampers: Modeling and dynamic performance considerations*. Engineering Structures, 2002. **23**(3): p. 309-323.
45. Yang G, Spencer BF, Jung HJ and Carlson JD, *Dynamic modeling of large-scale magnetorheological damper systems for civil engineering applications*. Journal of Engineering Mechanics, 2004. **130**(9): p. 1107-1114.
46. Mendis P, Ngo T, Haritos N, Hira A, Samali B and Cheung John CK *Wind loading on tall buildings*. Electronic Journal of Structural Engineering, Special Issue: Loading on Structures, 2007.p. 41-54.
47. Li HN, Liu Y, Li C and Zheng XW, *Multihazard fragility assessment of steel-concrete composite frame structures with buckling-restrained braces subjected to combined earthquake and wind*. The Structural Design of Tall and Special Buildings, 2020. **e1746**: p. 1-19.
48. Luongo A and Zulli D, *Parametric, external and self-excitation of a tower under turbulent wind flow*. Journal of Sound and Vibration, 2011. **330**(13): p. 3057-3069.
49. Anague Tabejieu LM, Nana Nbandjo BR and Filatrella G, *Effect of the fractional foundation on the response of beam structure submitted to moving and wind loads*. Chaos, Solitons and Fractals, 2019. **127**: p. 178-188.
50. Lin YK and Li QC, *Stochastic stability of wind excited structures*. Journal of Wind Engineering and Industrial Aerodynamics, 1995. **54/55**: p. 75-82.
51. Cai GQ and Wu C, *Modeling of bounded stochastic processes*. Probabilistic Engineering Mechanics, 2004. **19**(30): p. 197-203
52. Xie WC and Ronald MCSO, *Parametric resonance of a two-dimensional system under bounded noise excitation*. Nonlinear Dynamics, 2004. **36**(2-4): p. 437-453.
53. Fan FG and Ahmadi G, *Nonstationary Kanai-Tajimi models for El Centro 1940 and Mexico City 1985 earthquakes*. Probabilistic Engineering Mechanics, 1990. **5**(4): p. 171-181.
54. Moustafa A and Takewaki I, *Response of nonlinear single-degree-of-freedom structures to random acceleration sequences*. Engineering Structures, 2011. **33**(4): p. 1251-1258.
55. Ndemanou BP, Nana Nbandjo BR and Dorka U, *Quenching of vibration modes on two interconnected buildings subjected to seismic loads using magneto rheological device*. Mechanical Research Communication, 2016. **78**: p. 6-12.
56. Dyke SJ, Spencer BF, Sain MK and Carlson JD, *An experimental study of MR dampers for seismic protection*. Smart Materials and Structures, 1998. **7**(5): p. 693-703.

Appendix

$$b_1 = \int_0^1 \phi^2(X) dX, b_3 = \int_0^1 \phi''''(X) dX, b_4 = \int_0^1 \phi(X) dX,$$

$$\int_0^1 b_5 = \int_0^1 \phi^3(X) dX, b_6 = \int_0^1 \phi^4(X) dX, \sigma = \frac{b_4}{den}$$